

Electronic Communication in Linear Oligo(azobenzene) Radical Anions

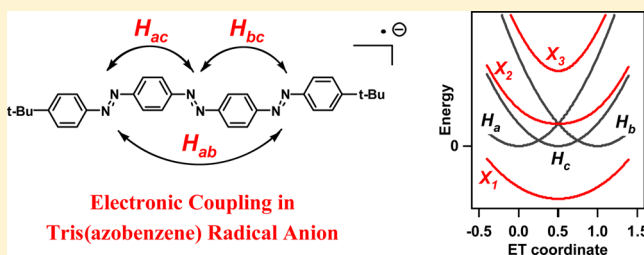
Álvaro Moneo,[†] Gonçalo C. Justino,[†] M. Fernanda N. N. Carvalho,[†] M. Conceição Oliveira,[†] Alexandra M. M. Antunes,[†] David Bléger,[‡] Stefan Hecht,[‡] and João P. Telo^{*,†}

[†]Centro de Química Estrutural, Instituto Superior Técnico, Universidade de Lisboa, Av. Rovisco Pais, 1049-001 Lisboa, Portugal

[‡]Department of Chemistry, Humboldt-Universität zu Berlin, Brook-Taylor-Strasse 2, 12489 Berlin, Germany

S Supporting Information

ABSTRACT: The radical anions of five bis(azobenzene) and one tris(azobenzene) compounds were studied by optical and electron paramagnetic resonance (EPR) spectroscopies in polar aprotic solvents. The radicals with planar or almost-planar bridges are charge-delocalized mixed-valence species. Localization of charge occurs only on radicals with highly twisted biphenyl bridges. The electronic coupling between the azobenzene charge-bearing units, calculated as half the energy of the intervalence band for the charge-delocalized and by the Hush equation for the charge-localized radicals, decreases with the distance and torsion angle between azobenzene units. These radicals have smaller electronic couplings between charge-bearing units than other mixed-valence organic radicals with similar bridges. However, the application of a three-stage model to the tris(azobenzene) radical anion intervalence band yields an electronic coupling between consecutive azobenzenes that is higher than in any of the bis(azobenzene) radicals studied.



INTRODUCTION

The azobenzene molecular unit has been extensively studied in the recent past due to the use of the cis–trans photoisomerization in optical switches,¹ information storage,² or optomechanical devices.³ These include not only single molecules with the azo group but also polymers containing the azobenzene unit, either in the main chain or as side groups. Additionally, the incorporation of the azobenzene rigid structure in several materials allows them to behave as photoresponsive liquid-crystal mesogens.⁴ Although the photochemistry of the azo group has received enormous attention, the potential use of azobenzene systems as charge carriers in organic devices has been seldom addressed in the literature. The intrinsic ability of a molecule to transport charge depends on the efficiency with which the charge moves within the π -conjugated system, and the use of mixed-valence chemistry offers a unique tool to study how the localization of charges in organic radical ions depends on the structural and chemical features.⁵ In this context, it is of significant interest to understand how the chemical structure affects the electronic coupling in negatively charged azobenzene oligomers.

Mixed-valence (MV) compounds are characterized by having two charge-bearing units (CBUs, often represented as M) symmetrically attached to a bridge (B), and being at an oxidation level for which the charges at the CBUs could be different. The Marcus–Hush two-state model⁶ uses parabolas representing the two diabatic states, each with the charge localized on one of the CBUs. These diabatic surfaces are allowed to interact through an electronic coupling term H_{ab} ,

producing the adiabatic energy surfaces shown as solid lines in Figure 1. The system is then described by two energies, the reorganization energy λ , which accounts for the vertical energy change of the CBUs upon electron transfer, and the electronic

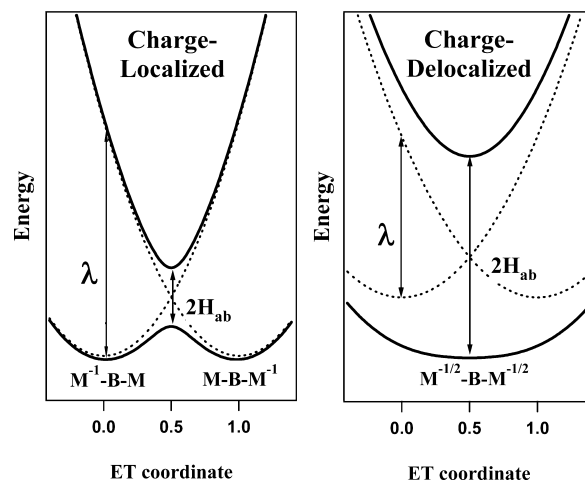


Figure 1. Two-state model Marcus–Hush diagrams for localized (left-hand side) and delocalized (right-hand side) mixed-valence radical anions.

Received: July 17, 2013

Revised: November 4, 2013

Published: November 28, 2013

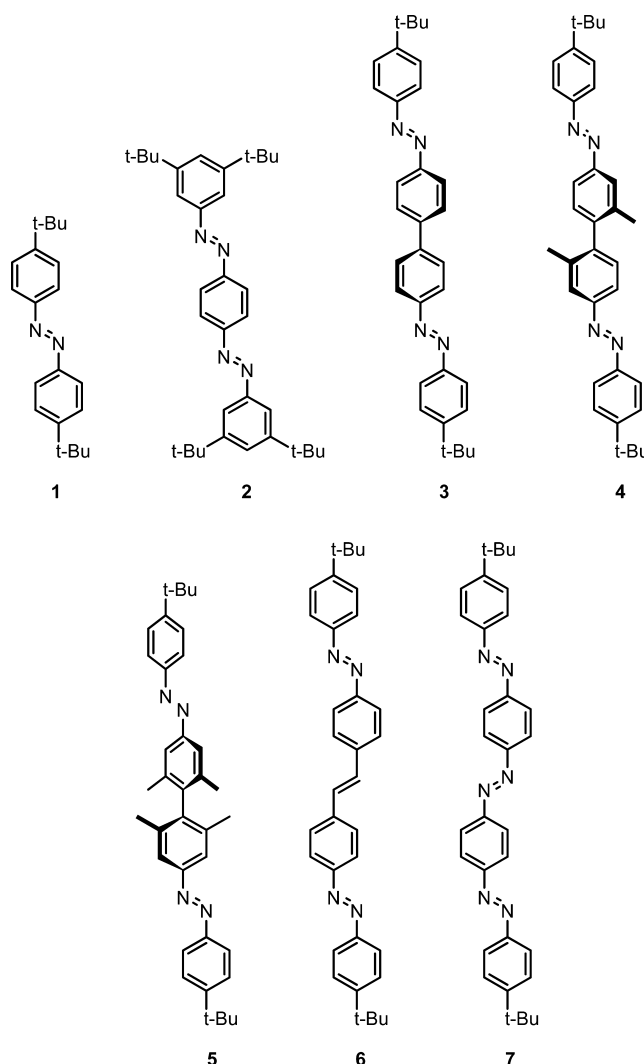


coupling H_{ab} . MV systems with large enough electronic couplings between CBUs are charge-delocalized, because the ground-state adiabatic energy surface has one single minimum, as shown on the right-hand side of Figure 1. If, however, the electronic coupling is small, the system is charge-localized, the ground-state adiabatic surface has two minima and interconversion between the two minima corresponds to the thermally activated intramolecular electron transfer between CBUs (Figure 1, left-hand side).

Localized and delocalized mixed-valence compounds can usually be distinguished by their low-energy optical absorption band, frequently called the intervalence band. The vertical excitation on a charge-localized system occurs from the ground-state minimum to a steeply sloping area of the excited-state energy surface, producing wide bands with no vibrational fine structure and energy maxima that correspond to the reorganization energy λ (Figure 1). In delocalized systems the electronic transition (which equals $2H_{ab}$ in the two-state model) occurs from the ground-state minimum to the excited-state minimum and the optical bands are much narrower and often show vibrational structure. The transition from charge-localized to charge-delocalized (which are also called class II and class III, respectively, in the Robin–Day terminology)⁷ occurs at $\lambda = 2H_{ab}$, so MV compounds with $\lambda > 2H_{ab}$ are charge-localized and with $\lambda < 2H_{ab}$ are charge-delocalized.

The azobenzene radical anion has been studied by EPR spectroscopy since the early 1960s.⁸ The complexity and high line width of the spectra made its analysis somewhat difficult, but in 1991 Gerson and co-workers proved unequivocally by ENDOR spectroscopy that the coupling constants of the two ortho and the two meta hydrogen atoms in the phenyl groups are different, which implies restricted rotation around the nitrogen–phenyl bond.^{8d} The reduction of either the *cis* or the *trans* isomer of azobenzene always yields the more stable *trans* radical, because the N=N double bond is weaker in the radical than in the parent neutral molecule.⁹ Actually, the reduction of *cis*-azobenzene to its radical anion is considered to be responsible for the fast isomerization to the *trans* isomer, even by the effect of low electric fields in liquid crystals containing the azobenzene unit.¹⁰

In a previous work we studied the azobenzene-bridged mixed-valence radical anion of 4,4'-dinitroazobenzene. It was found to be delocalized in all aprotic solvents studied, whereas the 4,4'-dinitrostilbene radical, also with 11 bonds between CBUs, is localized in solvents that induce a high reorganization energy, like acetonitrile (MeCN).¹¹ The azo nitrogens lower the reduction potential for the bridge relative to that of the hydrocarbon bridges, and this is known to lower the donor-bridge energy gap in radical anions, which increases the electronic coupling.¹² Although there are several works that study the effects of the nature of the bridge on the properties of organic MV compounds, the same amount of effort has not been applied to the systematic study of the nature of the charge-bearing unit, and there is no reference to organic MV species where the azo unit has been used as the redox center. We study in this work the radical anions of azobenzene oligomers 1–7 (see Supporting Information and ref 19 for the synthesis), where the charge is mainly centered on the azo groups, by optical and EPR spectroscopies, to address how the chemical structure affects the electronic communication between azobenzene units.



RESULTS AND DISCUSSION

The radical anions were prepared by reducing the oligo-(azobenzenes) 1–7 with sodium amalgam in aprotic solvents and in the presence of cryptand[2.2.2] to sequester the sodium counterion, and their optical and EPR spectra were recorded. The low solubility of either the neutral compounds or the reduced species limits the range of solvents that can be used. Most of the compounds above are not soluble in the 0.1–1 mM concentration range needed to acquire good spectra in acetonitrile (MeCN), for example, and either the radical anion or the dianion of some species precipitate in less polar solvents such as THF or methylene chloride.

4,4'-Di-*tert*-butylazobenzene (1). The optical spectra of monoazo compound 1 in THF are shown in Figure 2. The spectra of the neutral shows the usual transitions for azo dyes: the π – π^* transition ($\lambda_{\text{max}} = 334$ nm, $\log \epsilon = 4.43$) and the n – π^* transition ($\lambda_{\text{max}} = 438$ nm, $\log \epsilon = 2.92$). The radical anion spectrum is shifted toward lower energies, as is common upon reduction. Figure 2 also shows TD-DFT calculations for the radical anion vertical excitations and includes the assignments of the configuration interaction (CI) for the transitions using Hooijink restricted open-shell nomenclature for optical bands of radical ions, which designates filled orbital to singly occupied orbital (somo) transitions as type A, and somo to virtual orbital transitions as type B.¹³ More specifically, type A_{*n*} transitions occur from $\beta(\text{homo}-n)$ to $\beta(\text{lumo})$, and B_{*n*}

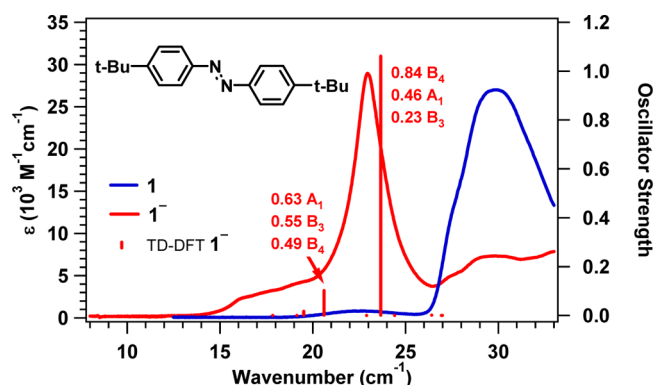


Figure 2. Optical spectra of the neutral (blue) and radical anion (red) of monoazobenzene **1** in THF. Sticks show TD-DFT calculated transition energies for the radical anion (UB3LYP/6-31+G*, PCM solvent model).

transitions from $\alpha(\text{homo})$ to $\alpha(\text{lumo}+(n-1))$. All transitions that do not involve $\alpha(\text{homo})$ or $\beta(\text{lumo})$ orbitals (generically abbreviated here as *somo*) are called C transitions. Neutral organic compounds typically have a bigger gap between their highest occupied molecular orbital (homo) and lowest unoccupied one (lumo) than between either filled or virtual orbitals. Addition of an electron gives a radical anion with a *somo* closer to the virtual orbitals than the filled ones, so the lowest energy transitions for radical anions are normally B type transitions. However, in the case of radical **1**[−] the B₁ transition is forbidden. The intense band at 23 000 cm^{−1} (435 nm, log ϵ = 4.46) is the sixth calculated transition, and the first five transitions with low or zero oscillator strength are probably responsible for the shallow and unresolved low-energy portion of the spectrum between 15 000 and 20 000 cm^{−1}.

The room temperature EPR spectrum of **1**[−] (Figure S1, Supporting Information) was simulated using different hyperfine coupling constants for the two ortho and the two meta hydrogens in each phenyl ring, which confirms that the rotation of the N–C bonds is slow, even at room temperature. The constants are similar to the ones published for radical anions of azobenzene derivatives.⁸

Charge-Delocalized Radical Anions. The optical spectra of bis(azobenzene) radicals **2**[−] and **3**[−] in THF are plotted in Figure 3. The lowest-energy band of **2**[−] is shifted to much lower energies than the ones of **1**[−], reflecting the increase in conjugation of the π -system. The bands of both spectra are narrow and show vibrational structure, showing that **2**[−] and **3**[−] are delocalized species. Spectra of the two radical anions in DMF show negligible shifts of the band maxima compared to THF. The transition energies of **3**[−] are significantly red-shifted as compared with the ones of **2**[−]. According to the two-state model of a delocalized system (Figure 1), the Marcus–Hush theory predicts that the maximum of the lowest-energy band, often called the intervalence band, occurs at $2H_{ab}$. Because the electronic coupling decreases markedly with distance, the compound with the longer distance between CBU's absorbs at lower energies.

Theoretical calculations show that both the neutral forms and the radicals can exist in two conformations, each corresponding to an energy minimum, as exemplified in Chart 1 for **2**. Gas-phase calculations show that the *s*-trans conformation of radical anion **2**[−] is more stable than the *s*-cis by 0.28 kcal/mol. A scan through the rotation around the bridge-azo bond (performed on the unsubstituted radical,

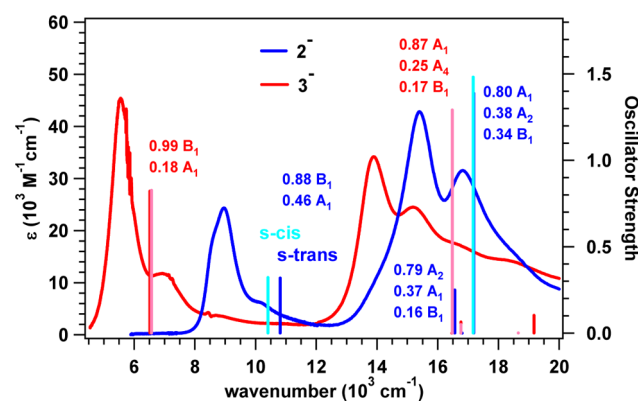


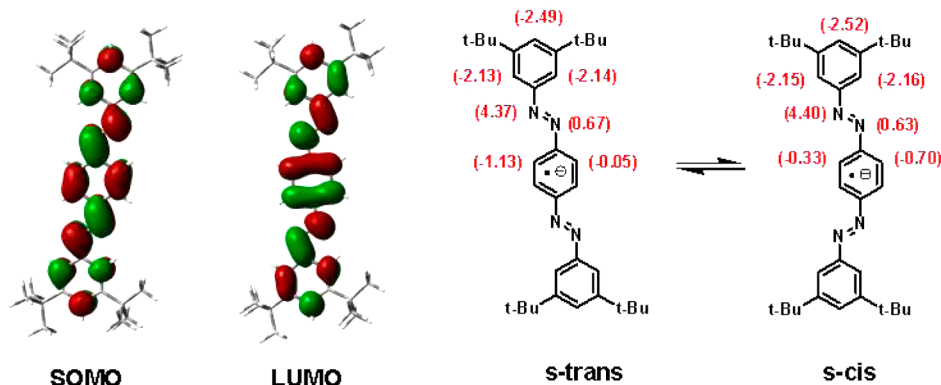
Figure 3. Optical spectra of **2**[−] (blue) and **3**[−] (red) in THF. Sticks show TD-DFT calculated transition energies (UB3LYP/6-31+G*, PCM solvent model) for the *s*-trans (dark colors) and *s*-cis (light colors) conformations. The assignment of the calculated transitions are shown only for the *s*-trans conformations.

where the *tert*-butyl groups were replaced by hydrogen atoms) shows a rotational barrier of 24 kcal/mol, whereas in the neutral compound it is only of 6.6 kcal/mol. This difference occurs because the double-bond character of the bridge-azo bond increases upon reduction, with the C–N bond length decreasing from 1.416 Å in neutral **2** to 1.395 Å in **2**[−]. This is caused by the extended conjugation of the unpaired electron and is the reason why the two ortho hydrogen atoms (and also the two meta ones) in **1**[−] and in azobenzene radical anion show different hyperfine coupling constants.⁸

TD-DFT calculations of the electronic transitions are shown as sticks in Figure 3, together with the main assignment of the transitions for the *s*-trans isomers. The most intense bands of the *s*-trans and *s*-cis conformations have nearly the same transition energies for both radicals, except in the case of the low energy band of **2**[−]. We therefore attribute the low energy shoulder on the first band of **2**[−] to the presence of the minor *s*-cis isomer. The calculations overestimate the energy of the transitions, as is usual for TD-DFT, but they do predict the relative intensity of the bands quite well. The low energy bands for both radicals have a strong B₁ character (*somo* to *lumo*), as found out for most radical anions.^{11,14}

The radical anion **2**[−] shows a complex EPR spectrum (Figure 4), but all the other radicals show only unresolved broad singlets (Figure S2, Supporting Information, as an example). The simulation of the EPR spectrum of **2**[−] proved to be a difficult task due to the superposition of lines and the small signal-to-noise ratio of the outer lines of the spectrum. We are reasonably sure about the presence of two pairs of very different nitrogen hyperfine coupling constants (4.12 and 0.32 G) and a 1.54 G constant corresponding to four equivalent hydrogen atoms. Adding extra coupling constants of 1.80 G (2H) and 1.20 G (2H) somewhat reproduces the experimental spectrum, but this simulation is still a poor match. We attributed this either to the presence of the minor isomer *s*-cis and the superposition of the two spectra or to the selective broadening of some lines due to the dynamic interconversion between the two species. Most of the calculated coupling constants of the *s*-cis isomer (Chart 1) are similar to the ones of the *s*-trans, and this might be the reason why we still see resolved lines, although with a reasonably high line width (0.35 G in the simulated spectrum). This may also suggest that one or more coupling constants are within the experimental line width. The

Chart 1. Single-Occupied Molecular Orbital (somo) and Lowest Unoccupied Molecular Orbital (lumo) Isosurfaces, s-cis and s-trans Equilibrium, and Gas-Phase Calculated Hyperfine Coupling Constants (Gauss) for 2^{-} ^a



^aThe constants symmetric with the presented ones are omitted.

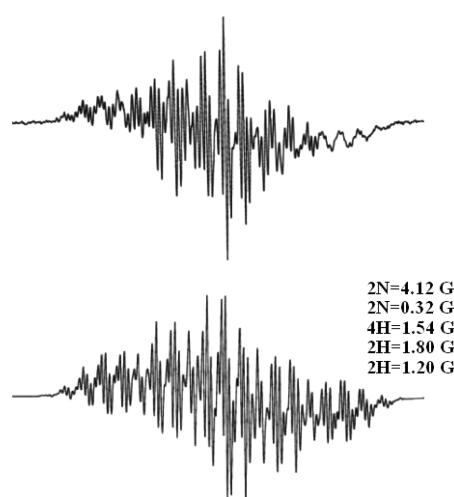


Figure 4. Room-temperature experimental EPR spectra of 2^{-} in THF (above) and tentative computer simulation (below) with hyperfine coupling constants shown.

calculated hyperfine constants on both isomers confirm that the coupling constant of the outer nitrogen atoms is significantly bigger than the one of nitrogens directly attached to the aromatic bridge.

The maximum of the lowest-energy optical band (E_{op}) occurs at 8950 cm^{-1} for 2^{-} ($\log \epsilon = 4.39$) and at 5530 cm^{-1} for 3^{-} ($\log \epsilon = 4.65$). These energies are lower than those of any of the other delocalized organic mixed-valence radical anions with the same bridges studied before. The energy maximum of the intervalence band is at $10\,820\text{ cm}^{-1}$ for the *p*-dinitrobenzene radical anion and at 6900 cm^{-1} for the 4,4'-dinitrobiphenyl radical anion, which are the dinitro equivalents of 2^{-} and 3^{-} ,¹⁴ and at even higher energies for the radical anions of *p*-dicyanobenzene and 4,4'-dicyanobiphenyl.¹⁵ The *p*-phenylene bridge unit of compound **2** causes normally large electronic couplings between charge-bearing units and most organic mixed-valence compounds with *p*-phenylene bridges are charge-delocalized and show E_{op} values larger than 2^{-} .¹⁶ Low H_{ab} values ($E_{op}/2$, according to the two-state model), and consequently often charge-localization, occur only in cases where the charge-bearing units are sterically forced out of the *p*-phenylene bridge plane, thus decreasing the conjugation between the CBUs and the bridge.^{17,18} However, theoretical

calculations show that radical 2^{-} has a planar π -system (Chart 1) and that 3^{-} has nearly planar azobenzene units (although the dihedral angle between rings in the biphenyl bridge is 22° , see below). As shown in Figure 4, the hyperfine coupling constants of the outer nitrogen atoms are more than 10 times bigger than the ones of the nitrogen directly attached to the bridge. We suggest that this spin distribution is the reason why the electronic coupling (and hence E_{op}) in these radicals is smaller than in other organic MV radicals with similar bridges.

The stilbene-bridge radical 6^{-} (Figure 5) has a longer conjugation path between CBUs than 3^{-} , so the energy of its

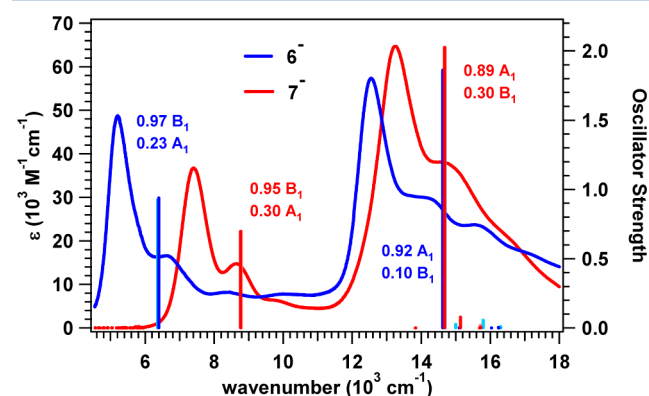


Figure 5. Optical spectra of 6^{-} (blue) and 7^{-} (red) in THF. Sticks show TD-DFT calculated transition energies for the s-trans (dark colors) and s-cis (light colors, but with very similar energies) conformations. The assignment of the calculated transitions are shown only for the s-trans conformations.

intervalence band (5200 cm^{-1} , Table 1) is shifted toward lower energies, reflecting the decrease of H_{ab} with distance. The intervalence band of tris(azobenzene) radical anion 7^{-} , however, appears at much higher energies (7400 cm^{-1}), although the distance between the outer azo units is nearly the same as in 6^{-} . This energy is even higher than the one of the intervalence transition in the biphenyl-bridged 3^{-} spectrum. The relative energies of the electronic transitions in Figure 5 are reasonably well predicted by TD-DFT calculations. The s-cis and s-trans conformations have nearly identical calculated energies for both radicals, and because the EPR spectra are unresolved broad signals, there is actually no experimental evidence that the two conformers coexist in solution.

Table 1. Band Parameters for the Low-Energy Band of Radical Anions from 2 to 7 and Difference between the First and Second Reduction Potentials (Energy Units cm^{-1})

radical	solvent	class ^a	E_{op}	ϵ_{max} ($\text{M}^{-1} \text{cm}^{-1}$)	$\Delta\bar{\nu}_{1/2}$ ^c	H_{ab}	ΔE (V)
2 ⁻	THF	III	8940 ^b	24300		4470 ^d	0.46 ^g
3 ⁻	THF	III	5560 ^b	45400		2780 ^d	0.18 ^g
4 ⁻	DMF	II	7600	1950	6450	770 ^e	0.12 ^g
	PhCN	II	7500	2050	6450	780 ^e	
5 ⁻	DMF	II	8300	300	7300	400 ^e	<i>g, h</i>
	PhCN	II	8200	250	6700	350 ^e	
6 ⁻	THF	III	5200 ^b	48500		2600 ^d	<i>h</i>
7 ⁻	THF	III	7400 ^b	36720		3700 ^d	0.27
						4770 (H_{ic}) ^f	

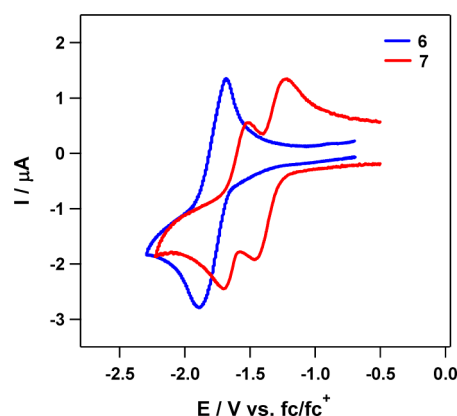
^aClass II are charge-localized and class III are charge-delocalized mixed-valence radicals. ^bValues in DMF are 50–200 cm^{-1} higher. ^cBandwidth at half-height of the delocalized band. ^dTwo-stage model value ($H_{\text{ab}} = E_{\text{op}}/2$). ^eFrom eq 3. ^fThree-stage model H_{ic} value with $\lambda = 5000 \text{ cm}^{-1}$ and $H_{\text{ab}} = 0$. ^gFrom ref 19. ^hSingle wave corresponding to 2 electrons.

Table 1 also shows the difference (ΔE) between the first two cathodic processes observed in compounds 1–7.¹⁹ ΔE is a measure of the degree of disproportionation of the radical anions into the neutral and dianion species (eq 1),

$$K_{\text{disp}} = [2-][0]/[\bullet-]^2 = \exp[-\Delta E^{\circ}(F/RT)] \quad (1)$$

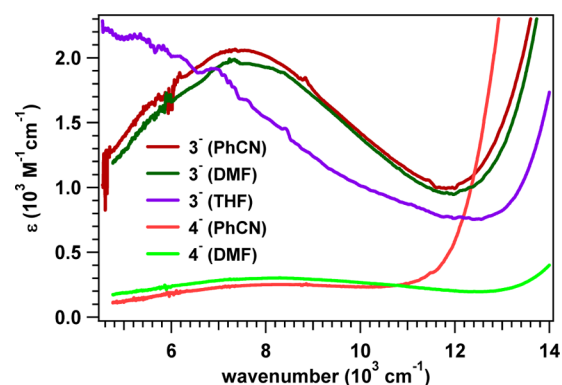
and can be correlated with the electronic coupling. ΔE decreases with the distance between CBUs, according to the predictable change in H_{ab} . Compound 6 displays a single cathodic process ($E_{1/2} = -1.79 \text{ V}$, vs Fc/Fc^+) at a potential slightly more positive than that corresponding to the reduction of mono(azobenzene) 1 (-1.96 V). By controlled-potential electrolysis, it was confirmed that the reduction of 6 involves two electrons per molecule. These data suggest a small electronic interaction between the two azobenzene units of 6⁻.

In contrast, compound 7 displays two well separated one-electron reductions processes at $E_{1/2} = -1.33 \text{ V}$ and $E_{1/2} = -1.60 \text{ V}$ (Figure 6) in agreement with a higher electronic

**Figure 6.** Cyclic voltammograms of 6 and 7 in $[\text{NBu}_4][\text{BF}_4]/\text{THF}$ (0.2 M). The cathodic wave of 6 corresponds to a two-electron reduction.

interaction than in 6⁻. In fact, ΔE values in Table 1 indicate that electronic coupling in 7 is higher than in 3 or 4, although lower than in 2 where electronic interactions are enhanced by close azo units.

Charge-Localized Radical Anions. Contrary to the other radicals, the optical spectra of the radical anions 4⁻ and 5⁻ show the wide and featureless Gaussian bands typical of localized mixed-valence species (Figure 7). The methyl groups

**Figure 7.** Low-energy portion of the optical spectra of 4⁻ and 5⁻.

force the central biphenyl bond to rotate, decreasing the electronic coupling of the bridge and inducing localization of charge. DFT calculations tend to overestimate delocalization and yield charge-delocalized structures for 4⁻ and 5⁻, which is not observed experimentally. Charge-localized structures were obtained for 4⁻ and 5⁻ using UHF/6-31G* gas-phase calculations, and so were for 3⁻, which is not correct in this case. More elaborate theoretical calculations get the right charge distribution for a significative number of MV compounds, but the size of our molecules prevents us from using them.²⁰ DFT calculations show the twist angle between phenyl rings in the biphenyl bridge of charge-delocalized 3⁻ to be 22° (36° in the charge-localized UHF calculation), whereas in the charge-localized 4⁻ and 5⁻ this angle increases to 88° and 90°, respectively (UHF calculations).

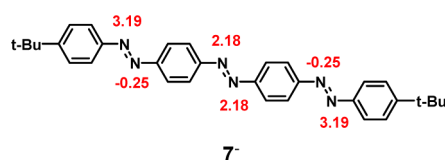
The energy maximum of the intervalence bands of localized radicals, which equals λ in the Marcus–Hush two-stage model, is very dependent on the solvent.^{6,11,14} However, a proper solvent study for 4⁻ and 5⁻ was limited by the low solubility of either the neutral or any of the charged species (radical anion or dianion). The only solvents that allowed us to obtain good results, DMF and PhCN, produce $E_{\text{op}} = \lambda$ values for organic radical anions that are very close to each other. A NIR band was also observed for 3⁻ in THF, although some precipitate was already obtained at this stage of reduction. THF induces smaller reorganization energies on MV radical anions and the maximum of the NIR band in this solvent seems to occur at energy values lower than the available window for this solvent. The band maxima for the 2,2'-dimethyl-4,4'-dinitrobiphenyl radical anion is at 11 000 cm^{-1} in DMF and at 10 500 cm^{-1} in PhCN, showing that the reorganization energy in 4⁻ is smaller

than in its dinitroaromatic equivalent.²¹ A more comprehensive analysis of the intervalence bands of these radicals will be presented below.

Electronic Couplings. According to the Marcus–Hush two-state model, the energy of the intervalence band of a delocalized mixed-valence compound corresponds to $2H_{ab}$, and the two-state model values of H_{ab} of all delocalized radicals are shown in Table 1. The H_{ab} values of 2^- , 3^- , and 6^- show the expected decrease with distance between CBUs, but the tris(azobenzene) radical 7^- has a two-state model electronic coupling (3700 cm^{-1}) much higher than the one of radical 6^- , although the distance between the outer azo units is nearly the same in both radicals. The two-state model assumes the superexchange mechanism, where the charge is transferred between CBUs by tunneling through virtual states of the bridge, so that the electron is at no time localized on the bridge. The electronic coupling H_{ab} depends on the energy gap between the CBU states and the bridge states, being bigger for bridges with the lUMO energy more close to the SOMO energy of the donor unit.¹² This would explain why the two-state H_{ab} value of 7^- is much higher than the one of 6^- . Introduction of the nitrogens in the bridge lowers its reduction potential relative to that of the hydrocarbon bridge, thus decreasing the bridge-CBU energy gap. The same effect was also found in the class III optical spectra of 4,4'-dinitroazobenzene and 4,4'-dinitrostilbene radical anions. Although the distance between nitro groups is also similar, the intervalence band E_{op} value of the azobenzene-bridged radical is 1.48 times that of the stilbene-bridge radical.¹¹

There is, however, a problem on applying the two-state model to radical 7^- . Although the EPR spectra are inconclusive, theoretical calculations at the UB3LYP/6-31G* level, which predict the nitrogen coupling constants reasonably well for 1^- and 2^- , give spin densities at the central azo group of 0.26 (sum of the two nitrogens). The spin density on each of the outer azo groups is only 0.18 (mostly on the nitrogen furthest from the bridge). The calculated coupling constants are shown in Chart 2.

Chart 2. Calculated Hyperfine Coupling Constants (Gauss) for 7^-



This means that the approximation of no significant electronic density on the bridge is no longer valid, and that 7^- actually behaves as a three-state model, having three diabatic surfaces corresponding to the charge localized on each of the three azobenzene units, as shown in Figure 8. For simplicity we retain the H_a and H_b designation for two diabatic energy surfaces with the electron located on each of the outer azobenzene units and add a third diabatic energy surface, H_c , corresponding to the charge located in the azobenzene bridge unit (which rigorously should not be designated as “bridge” in this case, but we will retain this designation). The energy and shape of the three diabatic parabolic surfaces should be very similar, because all the three correspond to reduced azobenzene units, so we will use degenerated surfaces with the same value of λ . According to the Marcus–Hush theory, these diabatic

surfaces interact through electronic coupling elements. As in the two-state model of Figure 1, H_{ab} corresponds to the direct electronic coupling between CBUs, but now a second electronic coupling $H_{ac} = H_{bc}$ (which we will simply call H_{ic} , with $i = a, b$) will express the interaction between the CBUs and the bridge. The system is described by the 3×3 secular determinant shown in eq 2, where E is the energy of the system. Equation 2 corresponds to a third-degree equation on E , whose solutions give rise to the three adiabatic energy states of the system.

$$\begin{vmatrix} H_a - E & H_{ic} & H_{ab} \\ H_{ic} & H_c - E & H_{ic} \\ H_{ab} & H_{ic} & H_b - E \end{vmatrix} = 0 \quad (2)$$

Analytical solutions of eq 2 are obviously difficult to get, and we used a numerical method to obtain the adiabatic states X_1 , X_2 , and X_3 (see Supporting Information for calculation details). Figure 8 shows the energy of the system for $\lambda/2H_{ic}$ values of 10, 2.5, and 1, with zero electronic coupling between charge-bearing units ($H_{ab} = 0$). For high $\lambda/2H_{ic}$ ratios, the ground-state energy surface (X_1) has three minima, although the central minimum (at $x = 0.5$) is always deeper (left-hand side of Figure 8). At approximately $\lambda/2H_{ic} < 5.2$ the ground state has only one minimum at $x = 0.5$ and the system becomes charge-delocalized.

In this case the energy of the first electronic transition is the difference between X_1 and X_2 at $x = 0.5$. At $1.5 < \lambda/2H_{ic} < 5.2$ the system, although delocalized at the ground state, has a double-minimum first excited state (central diagram of Figure 8). This corresponds to an excited-state mixed-valence case, which were extensively studied by Nelsen and Zink.²² At lower $\lambda/2H_{ic}$ values all three adiabatic states have only one minimum at $x = 0.5$. The fact that the first excited-state X_2 always equals $\lambda/4$ at $x = 0.5$ (the crossing point of the H_a and H_b diabatic states) is a consequence of assuming $H_{ab} = 0$. Allowing some direct interaction between CBUs ($H_{ab} > 0$) lowers X_2 ($X_2 = \lambda/4 - H_{ab}$ at $x = 0.5$) and decreases E_{op} . We need extra assumptions to estimate the values of λ , H_{ic} and H_{ab} by fitting the three-stage model to the intervalence band of 7^- ($E_{op} = 7400\text{ cm}^{-1}$). The reorganization energy, which is the vertical change in energy of the CBU (the azobenzene moiety in this work) upon reduction, is $7550\text{--}8250\text{ cm}^{-1}$ for the localized radicals 4^- and 5^- , but it is known that λ decreases with delocalization.^{11,14} For the delocalized radicals described above $\lambda < 2H_{ab}$, so the reorganization energy for each one should be smaller than $E_{op} = 2H_{ab}$. We suggest then that the reorganization energy for 7^- should be smaller than the smallest E_{op} value of Table 1 (5200 cm^{-1} for radical 6^-). We expect the bridge-CBU coupling H_{ic} to be similar to the H_{ab} value for 2^- , because both correspond to a coupling between azo groups through a *p*-phenylene bridge. Figure 9 shows the results of the fitting for three values of H_{ab} .

For a given value of H_{ab} , the CBU-bridge electronic coupling H_{ic} does not change much with λ in the range of values considered. Using lower λ values increases H_{ic} only slightly. Allowing direct electronic interaction between CBUs ($H_{ab} > 0$) increases H_{ic} by roughly the H_{ab} value. If we assume $H_{ab} = 0$ at first approximation, $H_{ic} = 4770\text{ cm}^{-1}$ for $\lambda = 5000\text{ cm}^{-1}$, which is close to the $H_{ab} = 4450\text{ cm}^{-1}$ value for 2^- . This corresponds to a highly delocalized case, similar to the one shown on the right-hand side of Figure 8. The second electronic transition

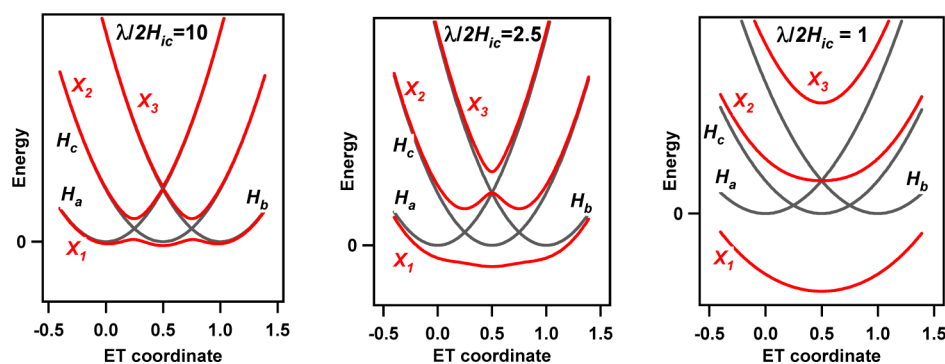


Figure 8. Marcus–Hush diagrams for a degenerated three-state model with different $\lambda/2H_{ic}$ ratios and zero electronic coupling between charge-bearing units ($H_{ab} = 0$).

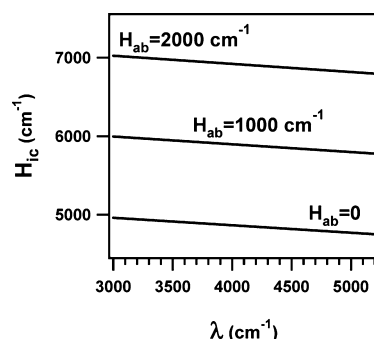


Figure 9. Results of the three-stage model fitting to the intervalence band energy maximum of 7^- .

(from the ground-state X_1 to the second excited-state X_3) is predicted by these values to be at $13\,550\text{ cm}^{-1}$, almost exactly at the absorption maximum of the second band of 7^- ($13\,240\text{ cm}^{-1}$). However, $X_1 \rightarrow X_3$ is a B_n type transition ($n > 1$), and according to the TD-DFT coefficients in the CI expansions, the only allowed transition of the first six with a main B type character is B_1 , so we suggest that $X_1 \rightarrow X_3$ either is forbidden or has a low oscillator strength. These results show that the electronic coupling between azobenzene units in tris-(azobenzene) 7^- is at least 4770 cm^{-1} , being much higher if we consider $H_{ab} > 0$. This value is larger than in any of the other bis(azobenzene) radicals. We claimed before that the electronic coupling in 2^- is smaller than in radicals with similar bridges due to the concentration of spin in the outer nitrogens of the two azo groups. This does not happen in 7^- . Due to the symmetry of the molecule, the spin densities on each of the

nitrogen atoms of the central azo group have to be the same. As shown in Chart 2, the calculated nitrogen coupling constants of the outer nitrogen atoms (3.19 G) are still much bigger than the ones of the nitrogens attached to the *p*-phenylene bridges (-0.25 G), but now both constants of the central azo group have also reasonably high values (2.18 G), and this should increase the coupling between azobenzene units.

Hush proposed that the electronic coupling of a localized MV compound could be extracted from the intervalence band shape according to eq 3

$$H_{ab} = 0.0206(\epsilon_{\max}\Delta\nu_{1/2}\lambda)^{1/2}/d_{ab} \quad (3)$$

where ϵ_{\max} is the maximum intensity, $\Delta\nu_{1/2}$ is the width at half-height, λ is the energy maximum of the band (E_{op}), and d_{ab} is the diabatic electron-transfer distance. The intervalence band parameters for 4^- and 5^- are shown in Table 1. However, the experimental values of ϵ_{\max} shown are not the real ones, because according to ΔE and eq 1, the maximum fraction of radical anion obtained under electrochemical conditions is 0.85 for 4^- due to the disproportionation of the radical anion into the neutral and dianion species. In the case of 5^- the two reduction waves are merged and an accurate measure of ΔE is impossible, but we estimate a maximum value of $\Delta E < 0.05\text{ V}$, so the maximum fraction of radical anion during reduction should be smaller than 0.57. Disproportionation is favored under electrochemical conditions, because ion-pairing with the 0.1 M electrolyte stabilizes the dianion preferentially to the radical anion or the neutral, decreasing $\Delta E = E_2 - E_1$.²³ Under the conditions used for the optical spectra, reduction produces only one sodium ion per radical anion and the presence of the

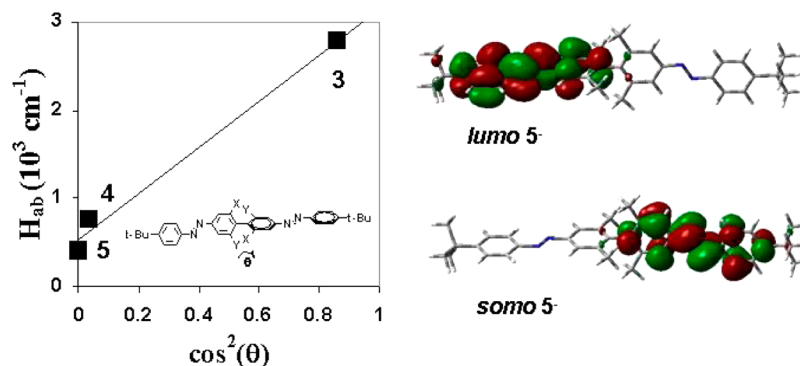


Figure 10. Dependence of H_{ab} on the twist-angle between rings for 3^- ($X = Y = \text{H}$), 4^- ($X = \text{H}$, $Y = \text{CH}_3$), and 5^- ($X = Y = \text{CH}_3$), and frontier orbitals for 5^- (UHF/6-31G*).

cryptand strongly disfavors ion pairing. Unfortunately, the optical spectra of the neutral form, the radical anion, and the dianion are not separated enough to balance the relative amount of the three species and there is no simple way of estimating K_{disp} in our case, so we used the fractions of the radical anion mentioned above to correct the ϵ_{max} values used in eq 1. The electron-transfer distances on the diabatic surfaces can be estimated through the change in dipole moment upon electron transfer according to the published procedure.²⁴ The d_{ab} values used here were 9.0 Å for 4^- and 9.1 Å for 5^- , obtained from the UHF/6-31G* localized structure dipole moments. The electronic couplings calculated from eq 1 are $H_{\text{ab}} = 770\text{--}780\text{ cm}^{-1}$ for 4^- and $H_{\text{ab}} = 350\text{--}400\text{ cm}^{-1}$ for 5^- , although one should be aware of the significant approximations used to calculate these values. H_{ab} decreases in the series 2^- to 4^- to 5^- , which reflects the increase of the torsion angle of the biphenyl bridge with the degree of methyl substitution. The electronic coupling is predicted to depend on $\cos^2(\theta)$, where θ is the twist angle between any of the p orbitals along the conjugation path. Although the number of points is limited, a plot of H_{ab} versus $\cos^2(\theta)$ for the radical anions of **3**, **4**, and **5**, where θ is the calculated dihedral angle between the aromatic rings, is shown in Figure 10. One should note that, as was found for dicyano radical anions with the same bridges,¹⁵ the electronic coupling is not zero for 5^- , even though the two phenyl rings of the bridge are orthogonal. Although the electronic density is almost completely located in one azobenzene moiety in the soma of 5^- , the 2' and 6' carbon atoms of the other azobenzene share a small fraction of the electronic density, which may provide a channel for electron transfer.

CONCLUSIONS

The bis(azobenzene) radicals studied in this work have smaller electronic couplings (H_{ab}) between azobenzene units than most of the other organic mixed-valence compounds with similar bridges due to an accumulation of spin density in the nitrogen atoms of the azo groups farthest from the bridge. H_{ab} values show the usual decrease with distance between charge-bearing units and with the twist angle between phenyl rings in the biphenyl-bridged systems. The reorganization energy of the charge-localized 2,2'-dimethylbiphenyl-bridged bis(azobenzene) radical 4^- is smaller than in the dinitro compound with the same bridge. Although with smaller H_{ab} and λ values, azobenzene mixed-valence compounds must have $\lambda/2H_{\text{ab}}$ ratios similar to dinitroaromatic radicals, because compounds of the two types with the same bridges show the same degree of charge localization. By applying a three-stage model to the intervalence band of the tris(azobenzene) radical anion 7^- , one obtains an electronic coupling between consecutive azobenzene units that is higher than in any of the bis(azobenzene) radicals studied here. Poly(*p*-phenylenevinylene) (PPV) is a conducting polymer used in light-emitting diodes and photovoltaic cells.²⁵ In poly(azobenzene), which is the azo equivalent of PPV, the azo bond will have a much higher tendency to localize the charge due to the electronegativity of the nitrogen atoms. However, this work predicts that poly(azobenzene) and its oligomers should also be good electronic conductors.

ASSOCIATED CONTENT

Supporting Information

Experimental techniques and synthetic procedures, theoretical calculations, NMR spectra, EPR spectra of 1^- and 7^- in THF, frontier orbitals, three-stage model calculations, and optimized structures of radical anions. This material is available free of charge via the Internet at <http://pubs.acs.org>.

AUTHOR INFORMATION

Corresponding Author

*J. P. Telo: e-mail, jptelo@ist.utl.pt.

Notes

The authors declare no competing financial interest.

ACKNOWLEDGMENTS

We thank the Fundação Para a Ciência e Tecnologia through its Centro de Química Estrutural and Projects PEst-OE/QUI/UIO100/2013 and PTDC/QUI-QUI/101433/2008. We thank the Portuguese MS Network (IST Node) for providing access to the facilities.

REFERENCES

- (1) (a) Ikeda, T.; Tsutsumi, O. *Science* **1995**, *268*, 1873. (b) Ichimura, K. *Chem. Rev.* **2000**, *100*, 1847. (c) *Molecular Switches*; Feringa, B. L., Ed.; Wiley-VCH: Weinheim, Germany, 2001.
- (2) Liu, Z. F.; Hashimoto, K.; Fujishima, A. *Nature* **1990**, *347*, 658.
- (3) (a) Natansohn, A.; Rochon, P. *Chem. Rev.* **2002**, *102*, 4139. (b) Hugel, T.; Holland, N. B.; Cattani, A.; Moroder, L.; Seitz, M.; Gaub, H. E. *Science* **2002**, *296*, 1103. (c) Bleger, D.; Yu, Z.; Hecht, S. *Chem. Commun.* **2011**, *47*, 12260.
- (4) (a) Cheng, L.; Torres, Y.; Lee, K. M.; McClung, A. J.; Baur, J.; White, T. J.; Oates, W. S. *J. Appl. Phys.* **2012**, *112*, 013513. (b) Hrozhyk, U. A.; Serak, S. V.; Tabiryan, N. V.; Hoke, L.; Steeves, D. M.; Kimball, B. R. *Opt. Express* **2010**, *18*, 8697. (c) Yan, Z.; Ji, X.; Wu, W. *Macromol. Rapid Commun.* **2012**, *33*, 1362.
- (5) (a) Hankache, J.; Wenger, O. S. *Chem. Rev.* **2011**, *111*, 5138. (b) Heckmann, A.; Lambert, C. *Angew. Chem., Int. Ed.* **2012**, *51*, 326.
- (6) (a) Marcus, R. A. *J. Chem. Phys.* **1956**, *24*, 966. (b) Marcus, R. A.; Sutin, N. *Biochim. Biophys. Acta* **1985**, *811*, 265. (c) Hush, N. S. *Prog. Inorg. Chem.* **1967**, *8*, 391. (d) Hush, N. S. *Coord. Chem. Rev.* **1985**, *64*, 135.
- (7) Robin, M. B.; Day, P. *Adv. Inorg. Radiochem.* **1967**, *10*, 247.
- (8) (a) Russell, G. A.; Janzen, E. G.; Strom, E. T. *J. Am. Chem. Soc.* **1962**, *84*, 4155. (b) Russell, G. A.; Konaka, R.; Strom, E. T.; Danen, W. C.; Chang, K. Y.; Kaupp, G. *J. Am. Chem. Soc.* **1968**, *90*, 4646. (c) Neugebauer, F. A.; Weger, H. *Chem. Ber.* **1975**, *108*, 2703. (d) Buser, U.; Ess, C. H.; Gerson, F. *Magn. Reson. Chem.* **1991**, *29*, 721.
- (9) (a) Laviron, E.; Mugnier, Y. *J. Electroanal. Chem.* **1978**, *93*, 69–73. (b) Grampp, G.; Muresanu, C.; Landgraf, S. *J. Electroanal. Chem.* **2005**, *582*, 171.
- (10) Tong, X.; Pelletier, M.; Lasia, A.; Zhao, Y. *Angew. Chem., Int. Ed.* **2008**, *47*, 3596–3599.
- (11) Nelsen, S. F.; Weaver, M. N.; Telo, J. P. *J. Am. Chem. Soc.* **2007**, *129*, 7036–7043.
- (12) (a) Wenger, O. S. *Inorg. Chim. Acta* **2011**, *374*, 3. (b) Hanss, D.; Walther, M. E.; Wenger, O. S. *Coord. Chem. Rev.* **2010**, *254*, 2584. (c) Newton, M. *Chem. Rev.* **1991**, *91*, 767.
- (13) (a) Hoijtink, G. J.; Weijland, W. P. *Recl. Trav. Chim. Pays-Bas* **1957**, *76*, 836. (b) Buschow, K. H. J.; Dieleman, J.; Hoijtink, G. J. *Mol. Phys.* **1963**, *7*, 1.
- (14) (a) Nelsen, S. F.; Konradsson, A. E.; Weaver, M. N.; Telo, J. P. *J. Am. Chem. Soc.* **2003**, *125*, 12493. (b) Nelsen, S. F.; Weaver, M. N.; Zink, J. I.; Telo, J. P. *J. Am. Chem. Soc.* **2005**, *127*, 10611. (c) Nelsen, S. F.; Schultz, K. P.; Telo, J. P. *J. Phys. Chem. A* **2008**, *112*, 12622.

- (15) Moneo, Á.; Carvalho, M. N. N.; Telo, J. P. *J. Phys. Org. Chem.* **2012**, *25*, 559.
- (16) Nelsen, S. F.; Weaver, M. N.; Telo, J. P.; Lucht, B. L.; Barlow, S. *J. Org. Chem.* **2005**, *70*, 9326.
- (17) (a) Nelsen, S. F.; Ismagilov, R. F.; Powell, D. R. *J. Am. Chem. Soc.* **1996**, *118*, 6313–6314. (b) Nelsen, S. F.; Ismagilov, R. F.; Powell, D. R. *J. Am. Chem. Soc.* **1997**, *119*, 10213–10222.
- (18) Telo, J. P.; Jalilov, A. S.; Nelsen, S. F. *J. Phys. Chem. A* **2011**, *115*, 3016.
- (19) Bléger, D.; Dokić, J.; Peters, M. V.; Grubert, L.; Saalfrank, P.; Hecht, S. *J. Phys. Chem. B* **2011**, *115*, 9930.
- (20) (a) Renz, M.; Kaupp, M. *J. Phys. Chem. A* **2012**, *116*, 10629. (b) Renz, M.; Kess, M.; Diedenhofen, M.; Klamt, A.; Kaupp, M. *J. Chem. Theory Comput.* **2012**, *8*, 4189. (c) Kaupp, M.; Renz, M.; Parthey, M.; Stolte, M.; Würthner, F.; Lambert, C. *Phys. Chem. Chem. Phys.* **2011**, *13*, 16973. (d) Renz, M.; Theilacker, K.; Lambert, C.; Kaupp, M. *J. Am. Chem. Soc.* **2009**, *131*, 16292.
- (21) Telo, J. P.; Nelsen, S. F.; Zhao, Y. *J. Phys. Chem. A* **2009**, *113*, 7730.
- (22) (a) Dibrelle, M.; Hoekstra, R.; Weaver, M. N.; Okadac, K.; Nelsen, S. F.; Zink, J. I. *J. Phys. Org. Chem.* **2012**, *25*, 578. (b) Lockard, J. V.; Valverde, G.; Neuhauser, D.; Luo, Y.; Weaver, M. N.; Nelsen, S. F.; J. I. Zink, J. I. *J. Phys. Chem. A* **2006**, *110*, 57. (c) Lockard, J. V.; Zink, J. I.; Konradsson, A. E.; Weaver, M. N.; Nelsen, S. F. *J. Am. Chem. Soc.* **2003**, *125*, 13471.
- (23) Macías-Ruvalcaba, N. A.; Evans, D. H. *J. Phys. Chem. B* **2005**, *109*, 14642.
- (24) Nelsen, S. F.; Newton, M. D. *J. Phys. Chem. A* **2000**, *104*, 10023.
- (25) (a) Spreitzer, H.; Becker, H.; Kluge, E.; Kreuder, W.; Schenk, H.; Demandt, R.; Schoo, H. *Adv. Mater.* **1998**, *10*, 1340. (b) Beek, W. J. E.; Wienk, M. M.; Janssen, R. A. *J. Adv. Mater.* **2004**, *16*, 1009.